Hindawi
International Journal of Antennas and Propagation
Volume 2024, Article ID 2945195, 15 pages
https://doi.org/10.1155/2024/2945195

Research Article

Design of Microstrip Antenna Arrays with Rotated Elements Using Wilkinson Power Dividers for 5 G Customer Premise Equipment Applications

Ting-Yi Huang and Yun-Jhang Lee

Department of Electrical Engineering, Feng Chia University, Taichung 407102, Taiwan

Correspondence should be addressed to Ting-Yi Huang; tyihuang@fcu.edu.tw

Received 13 September 2022; Revised 19 March 2024; Accepted 23 March 2024; Published 12 April 2024

Academic Editor: Hervé Aubert

Microstrip antenna arrays are proposed in this paper for the customer premise equipment (CPE) applications in the frequency range 1 (FR1) of the 5th generation (5 G) mobile networks. The proposed antenna arrays consist of three FR4 substrates. Antenna elements and feeding networks are optimized separately through parameter studies and then combined to form the proposed antenna arrays. Bandwidth-enhancing parasitic elements on the top substrate are broadside coupled to the microstrip antennas in the middle substrate, which are probe-fed by the microstrip feeding network using Wilkinson power dividers realized in the bottom substrate through the ground plane and the stud supporting air layer between the lower two substrates. Two antenna arrays, with four and eight antenna elements, are proposed for different gain specifications, 10 dBi and 12 dBi, respectively. Bandwidths of 10-dB return loss for both arrays fully covered the 5 G n78 frequency band (3.3–3.8 GHz). 20 dB isolation between antenna elements can also be achieved using the proposed layouts with rotated elements. The dimensions, radiation gain, and efficiency of the proposed antenna units, four-element array, and eight-element array are $65 \times 65 \times 11.4$, $115 \times 115 \times 11.4$, and $115 \times 215 \times 11.4$ mm^3, 6.2, 10.5, and 13 dBi, 74%, 56%, and 50%, respectively. The proposed antenna arrays exhibit the advantages of simple, low-cost, low-profile, and high-gain characteristics, which is potentially applicable to 5 G CPE outdoor unit (ODU)-related devices.

1. Introduction

The development of wireless communication systems has progressed rapidly in recent decades. The fifth generation new radio (5 G NR) system has been proposed to further enhance the bandwidth and capacity of the mobile communication system, including three major application scenarios defined as enhanced mobile broadband (eMBB), massive machine-type communications (mMTCs), and ultrareliable and low-latency communications (uRLLCs). To achieve the bandwidth enhancement, higher operation frequency bands were introduced, such as those in the sub-6 GHz frequencies (frequency range 1, FR1) or those in the even higher millimeter-wave frequencies (frequency range 2, FR2). On the other hand, capacity expansion is accomplished by smaller cell sizes that reduce the power of base stations to make frequency reuse more efficient and flexible. Compared to predecessor systems, the density of base stations in 5 G is significantly increased to complete the coverage of a certain area. The concept of customer premises equipment (CPE) is then proposed to ease the distribution of base stations, especially in metropolitan areas, by introducing customized, flexible, low-cost, and high bandwidth outdoor and/or indoor units (ODUs/IDUs) that bridge/route the 5 G mobile signals and the wireless local area networks (WLANs) without the need for wired connection.

A wide range of antennas and arrays can be found in the literature that are suitable for 5 G FR1 CPE ODU applications. Dual polarized antennas and arrays in the sub-6 GHz frequency bands can be used in cross polarized uplink/downlink configurations [1–4]. A 3–4.6 GHz dual

polarization antenna has been proposed using two orthogonal magneto-electric dipole antennas with an L-shaped feeding structure [1]. Isolation and half-power beamwidth were increased by adjusting dipole spacing and chamfered edge, respectively. 9 dBi peak gain and 20 dB front-to-back ratio have been achieved for a dual-polarized radiation pattern. A miniaturized microstrip antenna with a U-shaped parasitic element using coupled feeding has been proposed to decrease horizontal dimensions [2]. Broadside-coupled parasitic elements at certain height above the antenna have been proposed for the gain enhancement of a dual feed microstrip 2×2 antenna array [3]. A $\pm 45^{\circ}$ dual-polarized planar antenna array has been proposed for the applications of 2G/3G base stations using four folded dipoles [4].

Various techniques have been proposed to increase resonant modes, antenna gains, and directivities using parasitic elements [5–18]. Multiple stacked parasitic elements between the patch antenna and its ground plane can be used to achieve multipassband characteristics [5]. 8-dBi peak gain and 14-dB front-to-back ratio over a wide frequency band have been presented by adding parasitic elements around the patch antenna [6]. High-gain antennas such as a three-layer stacked patch antenna with 8.2-dBi peak gain and 21 dB front-to-back ratio in a small volume [7], probe-fed three-layer stacked patch antenna with 9.55 average gain and 26.5% fractional bandwidth [8], and a circularly polarized stacked patch antenna with 10.5 dBi gain [9] have also been proposed. Slot-coupled circularly polarized 2×2 antenna array with increased modes and directivity using four parasitic elements achieved gain enhancement of up to 10.5 dBi [10]. 2×2 antenna arrays using cross-shaped slot [11] and chamfered edge [12] for circular polarization also presented high gain characteristics, 11.6 and 17 dBi, respectively, using parasitic elements above their antennas. The gain increased from 18.7 to 20.5 dBi in the 4×4 antenna array proposed in [13] by stacking three layers of parasitic elements above its patch antenna array. Stacks of multilayer parasitic elements are also found in millimeter-wave antenna such as [14, 15] for high gain application. Multiple parasitic elements placed on the periphery of patch antenna have been proposed to form a 2×2 antenna array [16] and a 1×8 array [17]. A wideband patch antenna is accomplished by placing a parasitic element in the elliptic slot on the patch to increase the resonant modes and bandwidth [18].

Antenna arrays are commonly used in high-gain applications. L-band feeding networks using conventional Wilkinson power dividers with different dividing ratios from 2 : 1 to 16 : 1 have been proposed [19]. A low-profile 4×4 high gain antenna array in [20] presented a 1 dBi gain within a 1.6 mm thick substrate. 17 dBi gain is achieved in the 28-GHz frequency band using a 4×4 antenna array with vertical and horizontal half-power beamwidths 13.3° and 16.6°, respectively [21]. A left-hand circularly polarized 2×2 magneto-electric dipole array with a fractional bandwidth of 27.6% and a peak gain of 14 dBi at 29 GHz is proposed in [22]. A 4×4 coupled-fed multilayered antenna array using an L-shape feeding structure demonstrated a peak gain of 19.65 dBi [23]. Another 4×4 antenna array has been proposed to lower the side lobe level from −11.9 dB to −26.8 dB by adjusting the feeding network while maintaining its gain degradation within 0.6 dB [24]. A Chebyshev array has been proposed to minimize its side lobe level below −23.8 dB with a peak gain 24 dBi [25].

Research works related to the isolation between elements of antenna arrays are also important when dealing with miniaturization [26–30]. Decoupling vias are proposed in [26] which increase element-wise isolation such that the array size can be effectively reduced. A sequential phase feed network is proposed to achieve wide bandwidths for both impedance matching and axial ratio while reducing the coupling between antenna elements [27]. Different isolation structures such as electric bandgap structures, defected ground structures, capacitive elements, and neutralization lines have been studied in [28] to realize a MIMO antenna system with an isolation as high as 65 dB. An antenna array designed for the applications of base stations proposed in [29] decoupled two linear polarized antennas in H-plane and E-plane using metasurface such that the isolation levels were increased by 15 dB. Another base station antenna with compact size and dual-polarized broadband characteristic presented an isolation design using two symmetric shorting pins with respect to the feeding cable that improved the isolation between dual polarization to 40 dB [30]. A four-element stringray-shaped MIMO antenna system using rotated element and an isolation-improving structure at the center has also been proposed with improved spatial diversity and reduced mutual coupling for UWB applications [31].

Antennas and arrays for CPE applications in the sub-6 GHz frequency band are also popular recently [32–35]. Ultra-wideband monopole antenna [32] and planar trapezoidal monopole antenna [33] were proposed with isotropic radiation patterns for TVWS CPE. A dual-band antenna system using a two-element slot meander patch antenna is proposed to operate at 1.8 GHz and 2.6 GHz for LTE-WLAN CPE [34]. Another dual-band CPE application in the sub-6 GHz frequency band using slot antenna array can also be found in [35]. A hybrid antenna-in-package (AiP) system that covers multiple frequency bands in both sub-6 GHz and millimeter frequencies using slot antenna and an 8×8 antenna array, respectively, is presented for CPE IDU [36]. In 5 G CPE applications, 45° linearly polarized antennas are typically used. Dual polarized antennas with $\pm 45^{\circ}$ linear polarization are also proposed for diversity [37].

This paper proposes the design of simple, low-cost, and low-profile antenna arrays for 5 G CPE ODU applications using microstrip antennas with parasitic elements and feeding networks using Wilkinson power dividers, which provide 10–13 dBi gains in 5 G FR1 n78 (3.3–3.8 GHz) frequency band. Design of the proposed antenna is described in Section 2, including a description of the structure and parametric studies of the antenna element, the feeding network, and the proposed arrays with the aid of 3-dimensional full-wave solver Ansys HFSS. Comparison of simulated results and experimental verification and further discussion will be presented in Section 3, followed by a few conclusion remarks in the last section.

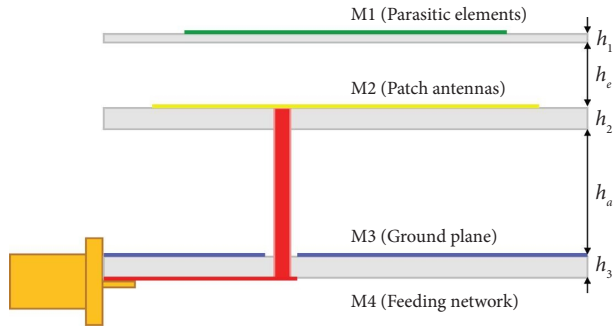

Figure 1: Layer stack up of the proposed antenna arrays (not in scale).

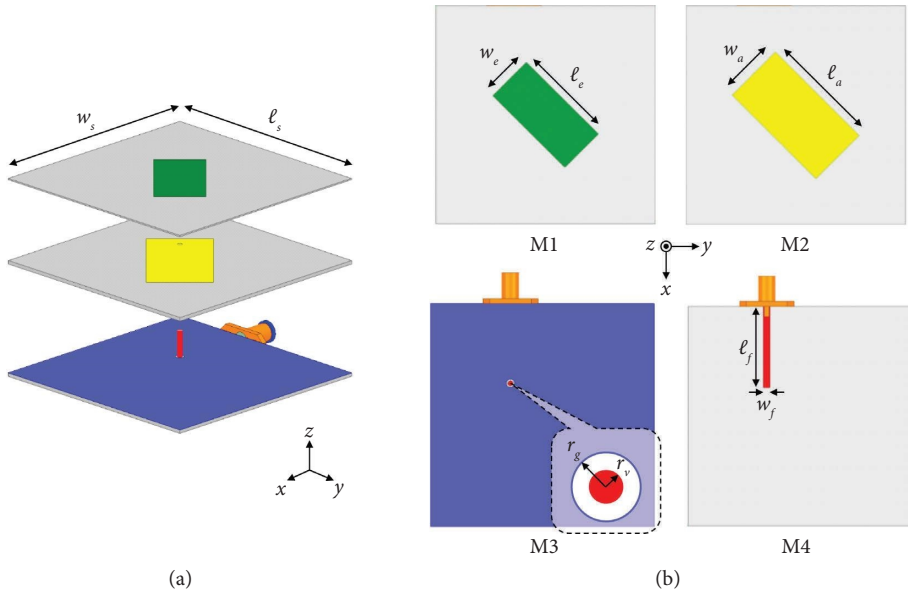

Figure 2: Structure of the proposed antenna unit. (a) Three-dimensional view. (b) Layouts at each metal layer.

2. Design of the Proposed Antenna Arrays

The proposed antenna arrays are realized in a layered structure consisting of three FR4 PCB substrate layers with air gaps supported by Nylon posts between the adjacent substrate layers, as shown in Figure 1. Four metal layers are used for the layouts of the proposed antenna arrays. The first metal layer, M1, on the upper side of the top substrate is used for parasitic elements. The microstrip patch antenna elements are placed in the second metal layer, M2, on the upper side of the center substrate. The third and fourth metal layers, M3 and M4, are the upper and lower sides of the bottom substrate, respectively. M3 is a fully covered metal layer acting as the common ground plane for both the patch antennas at M2 and the feeding network at M4. There are also through vias from M4 to M2 to perform the probe feeding from the feeding network to the antenna elements. The layer stack up has been optimized by following a similar procedure described in [38]. Design of the proposed antenna arrays consists of three parts. The design of proposed antenna units is presented first, followed by the design of feeding networks. A configuration of 45° rotated antenna units in the antenna arrays is also proposed to reduce mutual couplings without increasing the sizes of the arrays. Design results of the antenna unit with reduced mutual couplings and the feeding networks are then combined to realize the proposed antenna arrays.

2.1. Antenna Unit. As shown in Figure 2, the proposed antenna unit is formed by a microstrip rectangular patch antenna at M2 which broadside couples to another rectangular patch parasitic element right above it. The microstrip patch antenna is probe-fed using a cylindrical via structure through the antipad aperture in the ground plane (M3). The through via is then connected to a 50-Ω microstrip feeding transmission line at the bottom metal layer (M4), which is terminated by a surface mount adaptor (SMA) for experimental verification. The microstrip feeding transmission line will come from one of the output ports of the feeding networks in the design of antenna arrays. Related dimensions of the probe feeding structure are designed in a similar manner proposed by [38]. Parametric studies for the key design parameters of the proposed antenna unit are shown in Figures 3 and 4. Lengths of the microstrip patch antenna and the parasitic element, ℓ_a and ℓ_e, respectively,

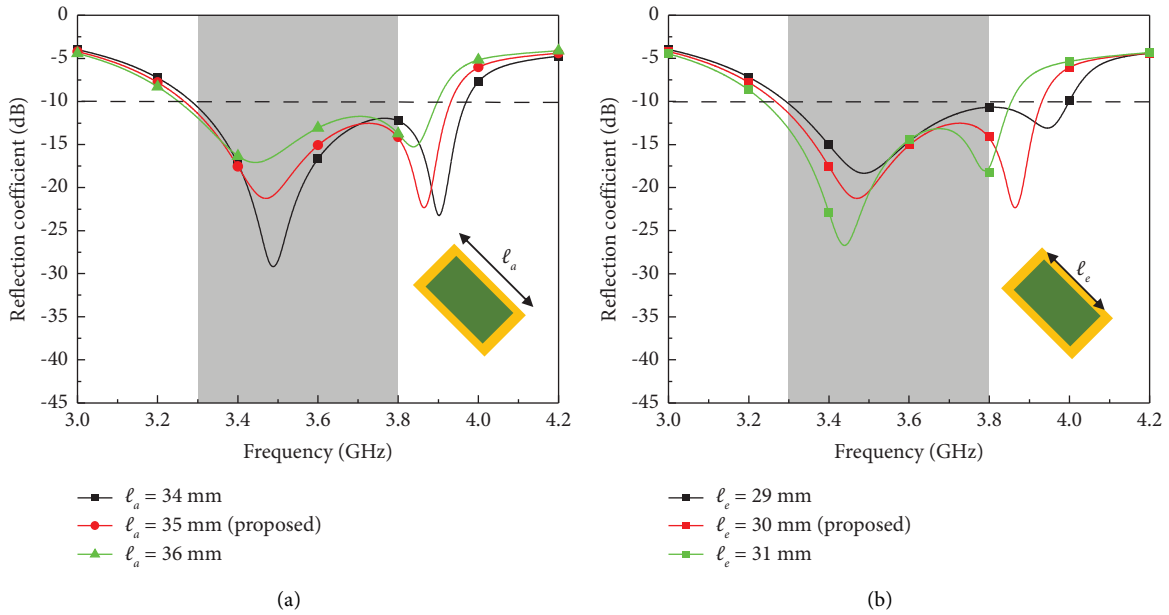

Figure 3: Adjusting the resonant modes by changing the lengths of (a) the microstrip patch antenna and (b) the parasitic element.

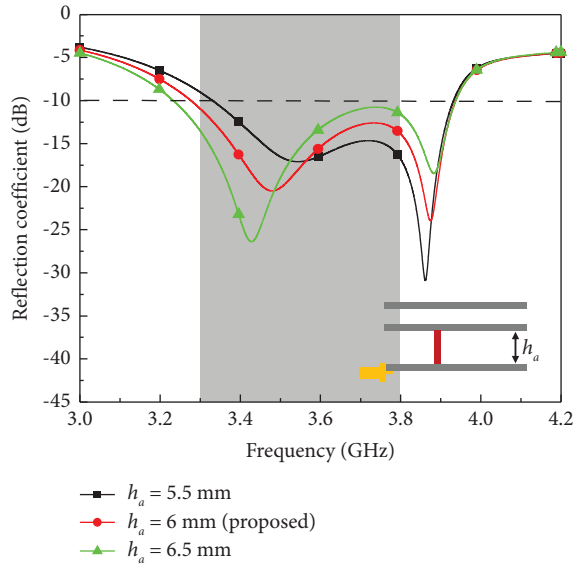

Figure 4: Adjusting the impedance matching by changing the separation between the microstrip patch antenna and its ground plane.

can be adjusted to control the lower and higher resonant modes of the proposed antenna unit. The separation between the antenna and its ground plane, h_a, can then be tuned to achieve impedance matching. The final design parameters are listed in Table 1.

2.2. Feeding Network. The feeding network of the proposed antenna arrays consist of successive power dividing stages. The Wilkinson power divider shown in Figure 5 is used as a basic building block, which are realized by following conventional design procedures [39]. Each of the output ports, port 2 and 3, is connected to another power divider in the next stage. Two- and three-stage H-tree patterns can thus be constructed for the feeding networks of the proposed 4-element (2×2) and 8-element (4×2) antenna arrays, respectively. As shown in Figure 5, return loss more than 20 dB, insertion loss less than 0.7 dB, and isolation below 25 dB can be achieved throughout the entire n78 frequency band.

2.3. Antenna Array. The proposed antenna arrays are realized by combining the previous design results. The feeding microstrip lines of the antenna units are connected to the output ports of the feeding structure. The mutual coupling between antenna units can be reduced by rotating individual antenna unit with respect to its feeding

Table 1: Final design parameters of the proposed antenna unit.

Parameter	Value (mm)
h_1	0.4
h_2	1.0
h_3	1.0
h_e	3.0
h_a	6.0
l_s	65
l_a	35
w_a	18
l_e	30
w_e	14
l_f	24
w_f	1.9
r_v	0.7
r_g	1.2

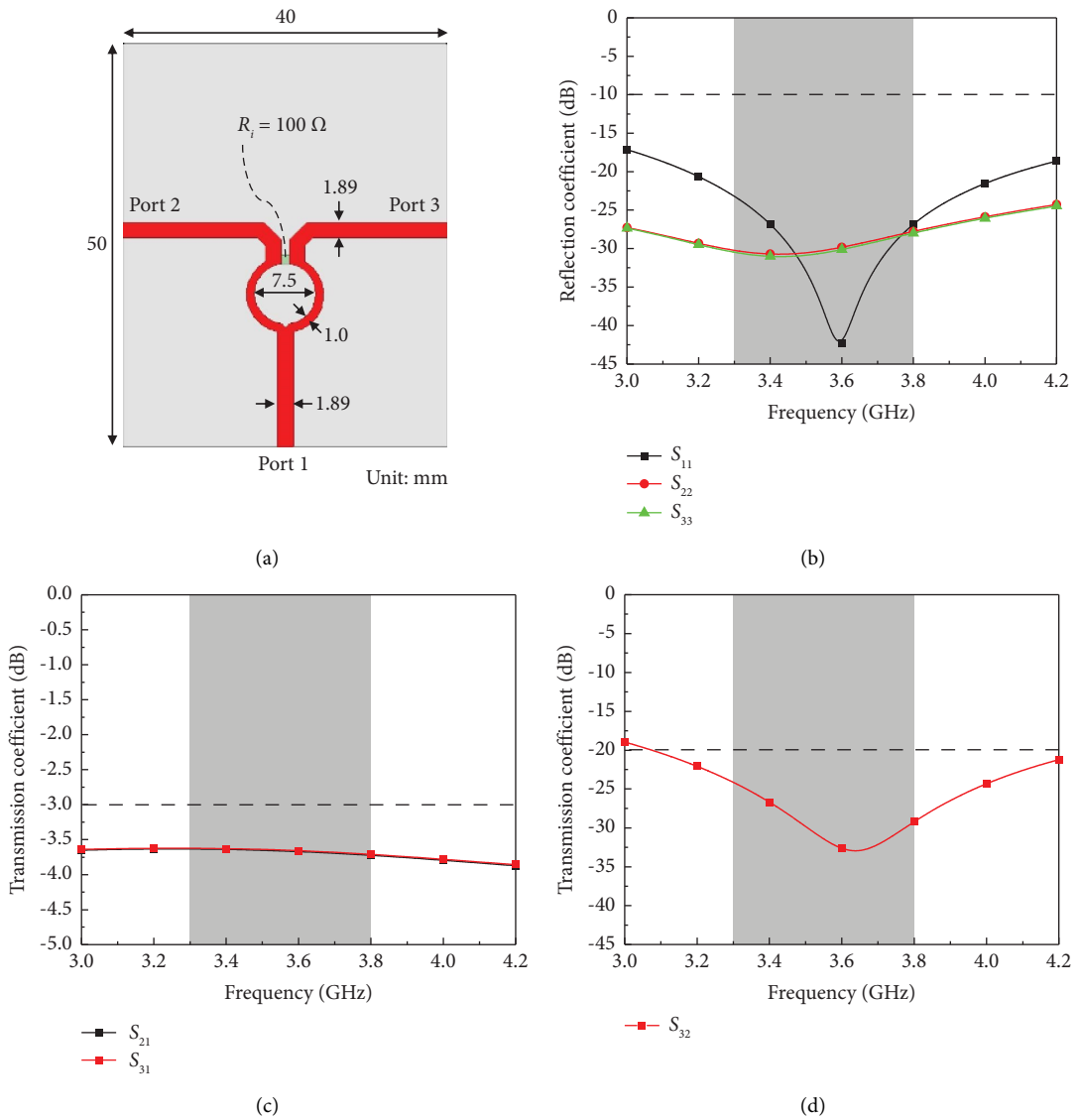

Figure 5: Wilkinson power divider used in the feeding network of the proposed antenna arrays. (a) Layouts and dimensions; (b) return loss; (c) insertion loss; and (d) isolation.

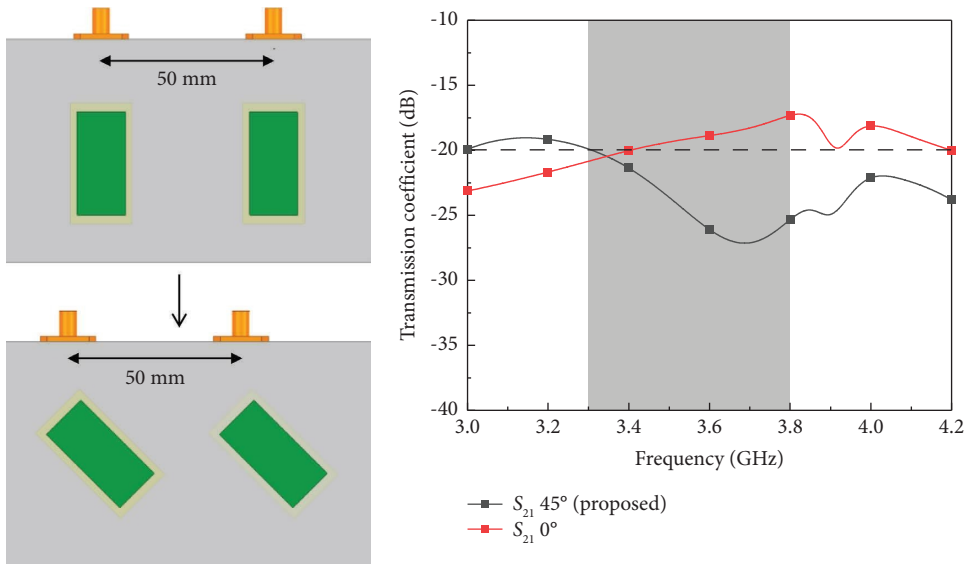

(a) (b)

Figure 6: (a) Rotating the antenna units in the antenna array to reduce mutual coupling. (b) Simulated results for different rotating angles.

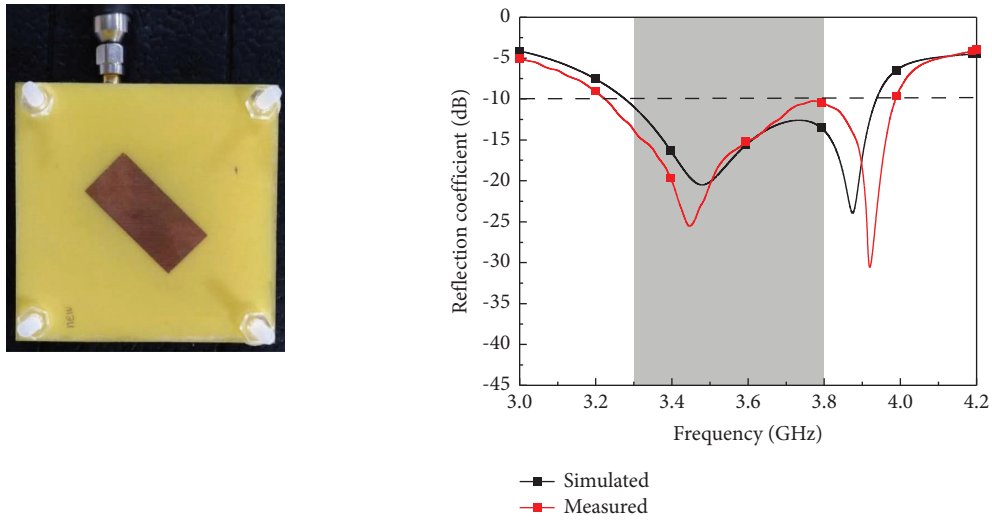

(a) (b)

Figure 7: Continued.

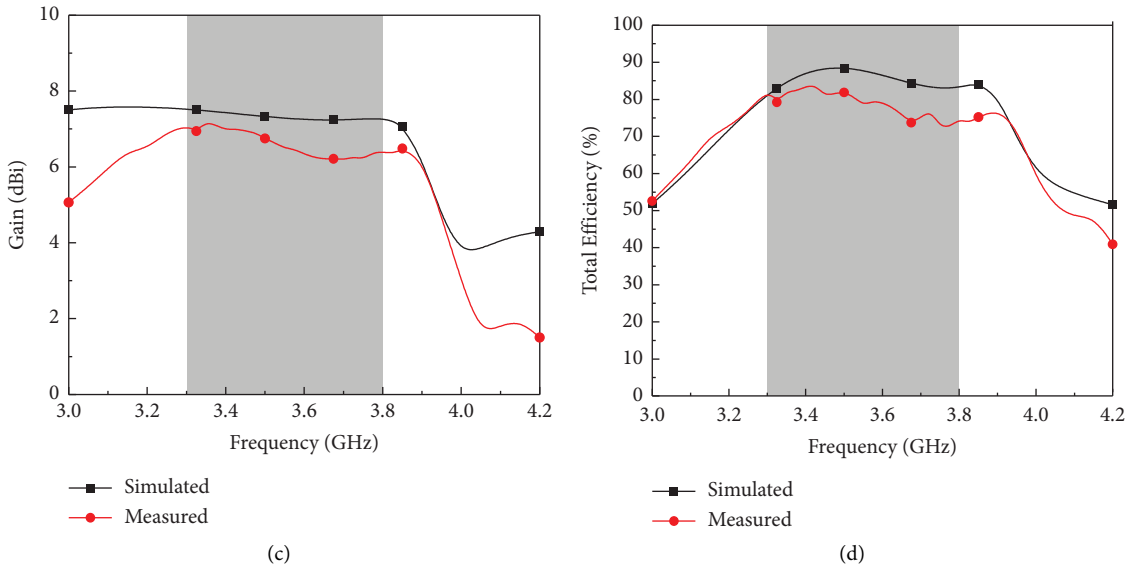

Figure 7: (a) Photo of the proposed antenna and its simulated and measured (b) return loss, (c) gain, and (d) efficiency.

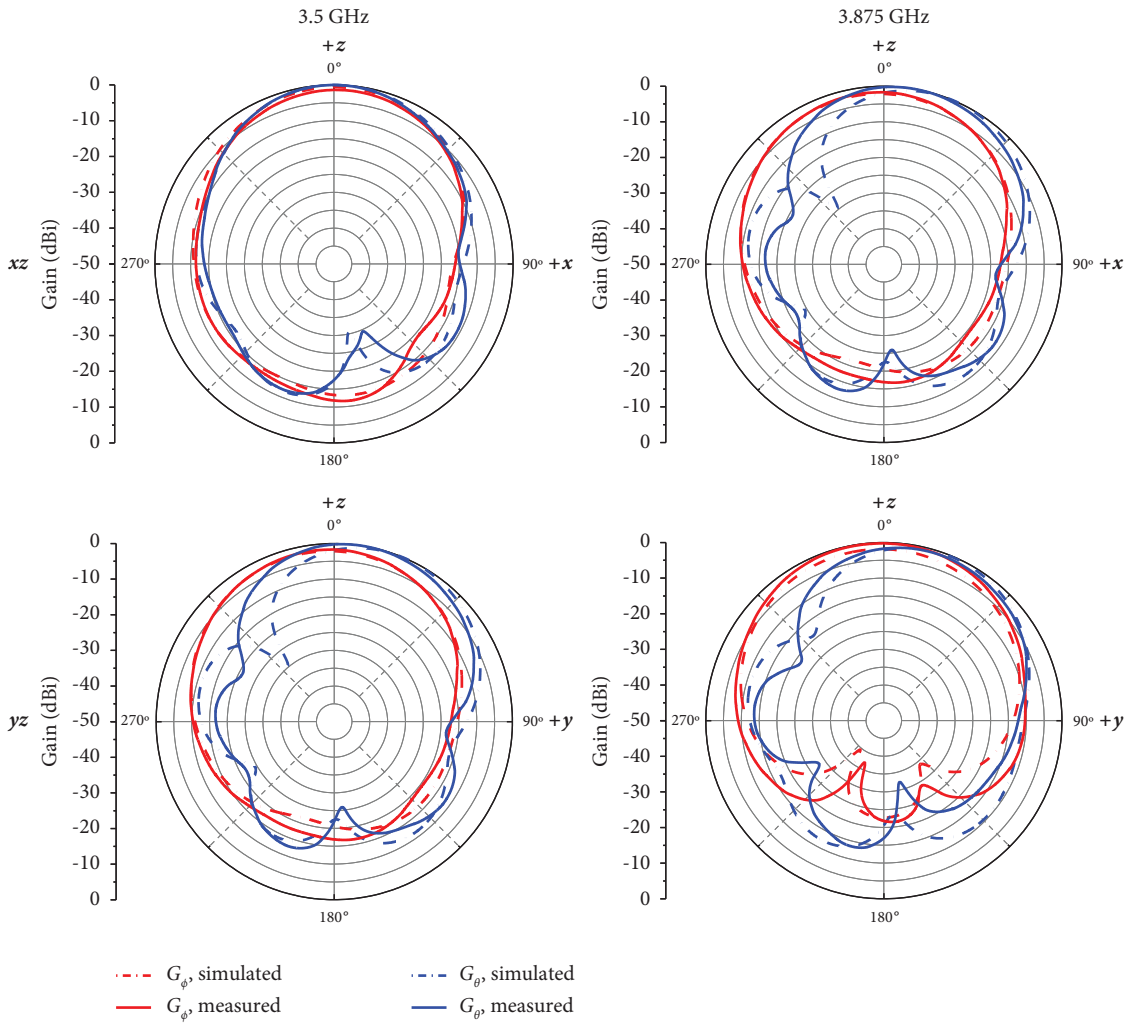

Figure 8: Simulated and measured radiation patterns of the proposed antenna at different planes and frequencies.

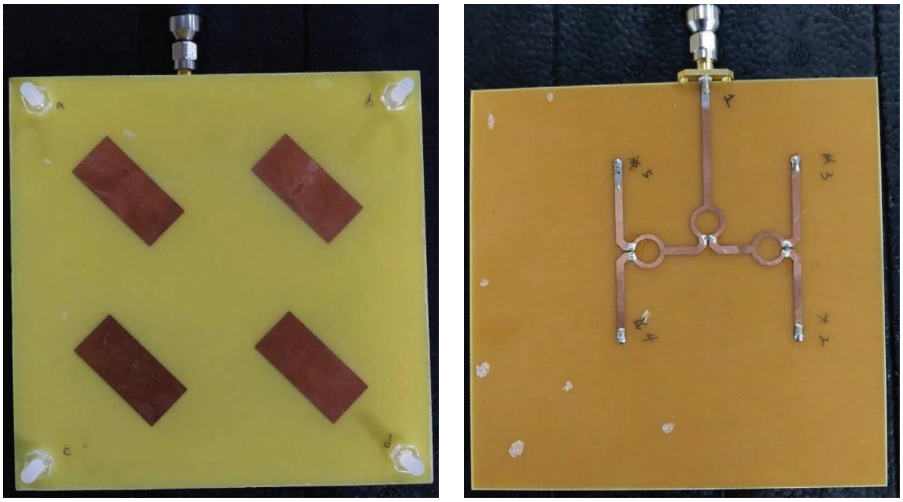

(a) (b)

Figure 9: Photo of the proposed 4-element antenna array on (a) the top side and (b) the bottom side.

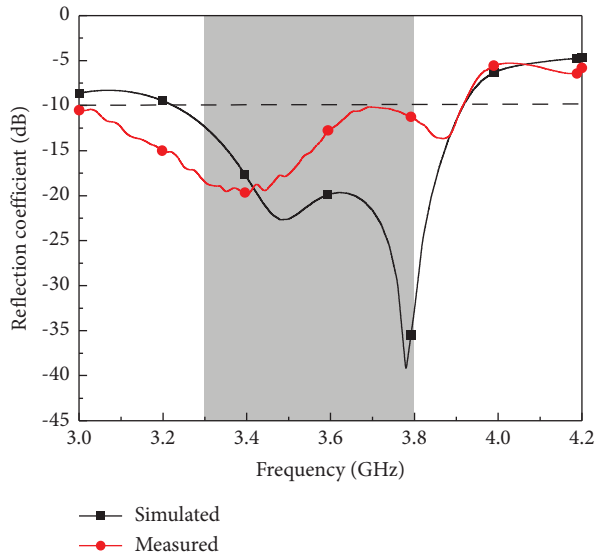

Figure 10: Simulated and measured reflection coefficients of the proposed 4-element antenna array.

probe, as shown in Figure 6(a), the minimum edge-to-edge distances between the units can be intuitively increased by a factor of $\sqrt{2}$ while the spacing between antenna units and the total sizes of the proposed arrays remain approximately the same, and the mutual thus coupling between adjacent units can be effectively reduced. Figure 6(b) shows that after a 45° rotation, the mutual coupling between the antenna units become less than 20 dB in the frequency range of interest.

3. Experimental Verification and Discussion

The proposed antenna unit, a four-element (2 × 2) array and an eight-element (4 × 2) array were fabricated to perform experimental verifications. Antenna gain and total efficiency have been measured using an automated over-the-air (OTA) compact antenna test range (CATR) measurement system [40], which was calculated in the same way as mentioned in [41–44]. The gain was calculated using Friss formula as follows:

$$G_2\ (\mathrm{d}B) = 20 \log_{10}\left(\frac{4\pi r}{\lambda}\right) + 10 \log_{10}\left(\frac{P_2}{P_1}\right) - G_1\ (\mathrm{d}B), \quad (1)$$

where G_2 and G_1 are the gains of the antenna under test and reference antenna, respectively. r is the distance between the antennas. λ is the wavelength. P_2 and P_1 are the received and transmitted power of the antenna under test and reference antenna, respectively. Total efficiency is calculated by

$$\text{Total efficiency} = \text{Radiation efficiency} \times \left(1 - |S_{11}|^2\right), \quad (2)$$

where

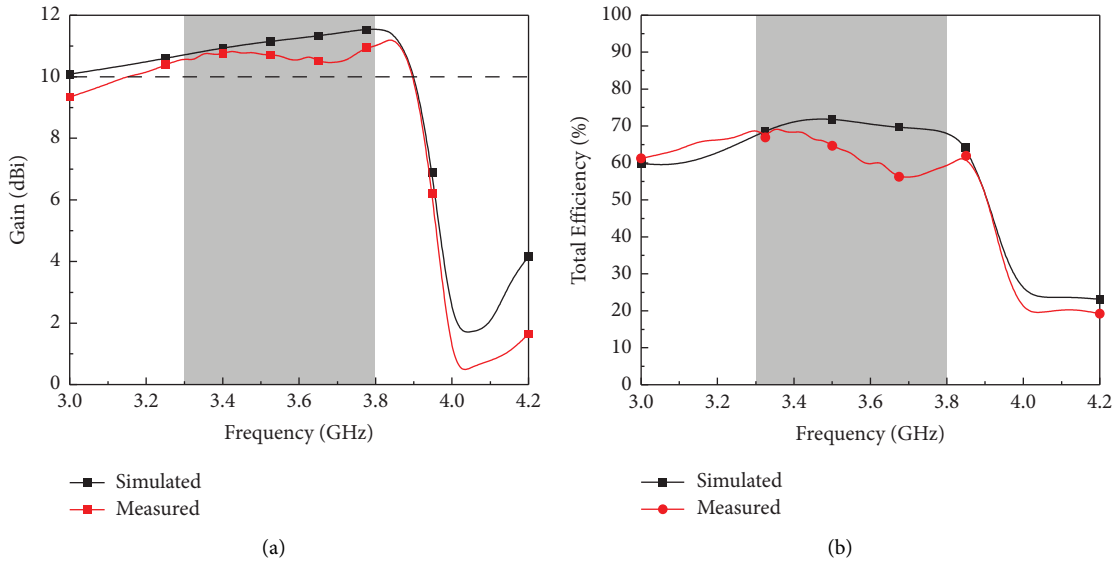

Figure 11: Simulated and measured (a) gain and (b) efficiency of the proposed 4-element antenna array.

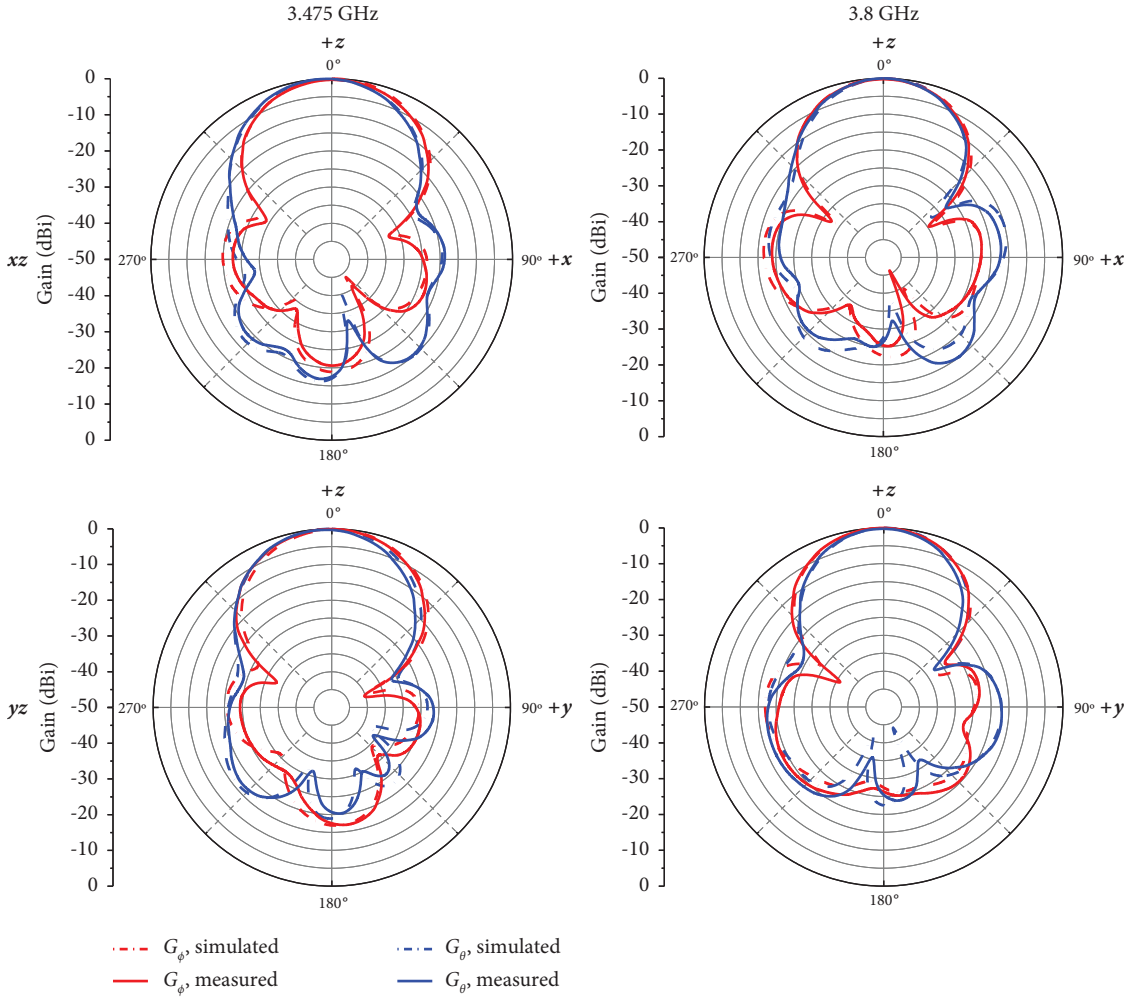

Figure 12: Simulated and measured radiation patterns of the proposed 4-element antenna array at different planes and frequencies.

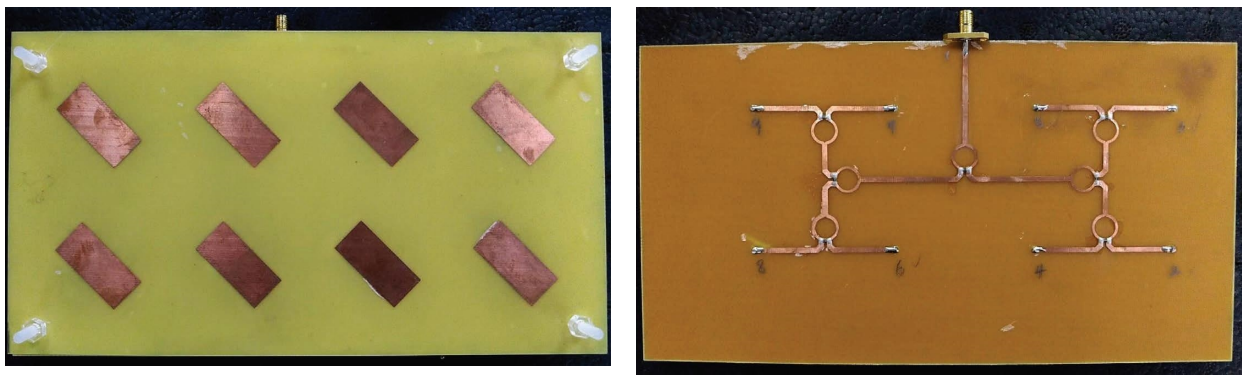

(a) (b)

Figure 13: Photo of the proposed 8-element antenna array at (a) the top side and (b) the bottom side.

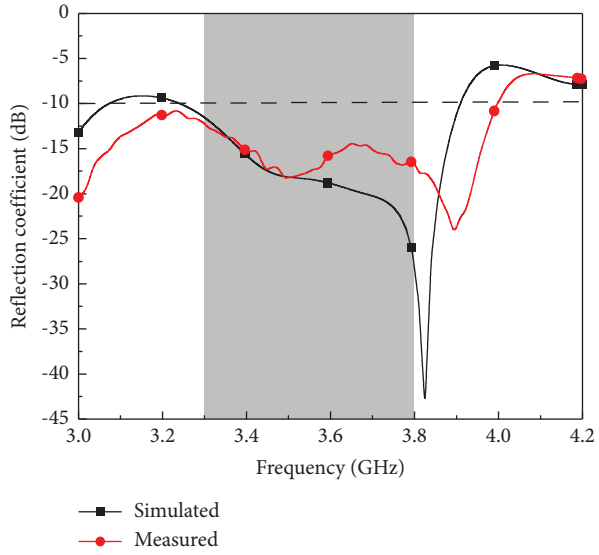

Figure 14: Simulated and measured reflection coefficients of the proposed 8-element antenna array.

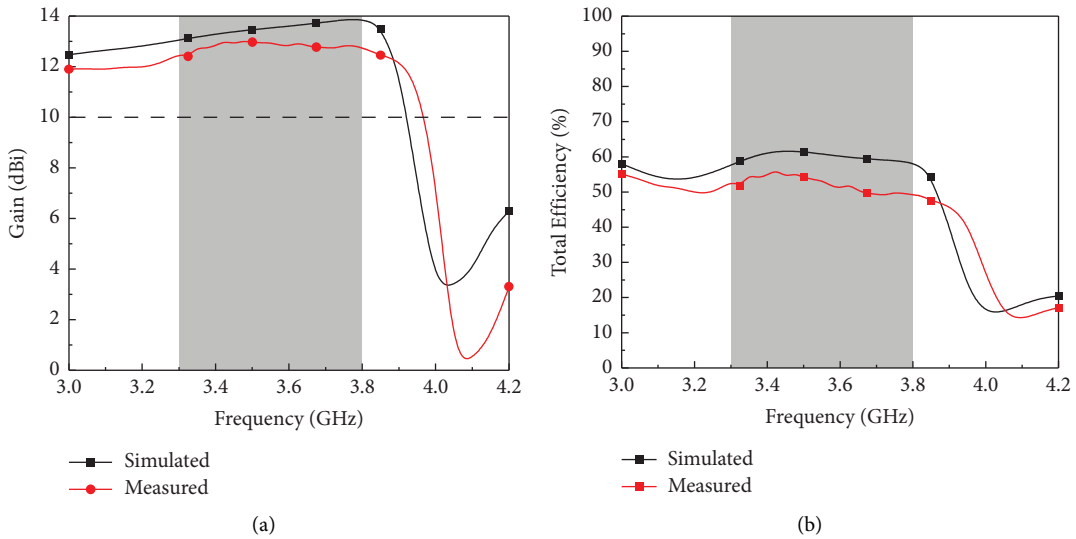

(a) (b)

Figure 15: Simulated and measured (a) gain and (b) efficiency of the proposed 8-element antenna array.

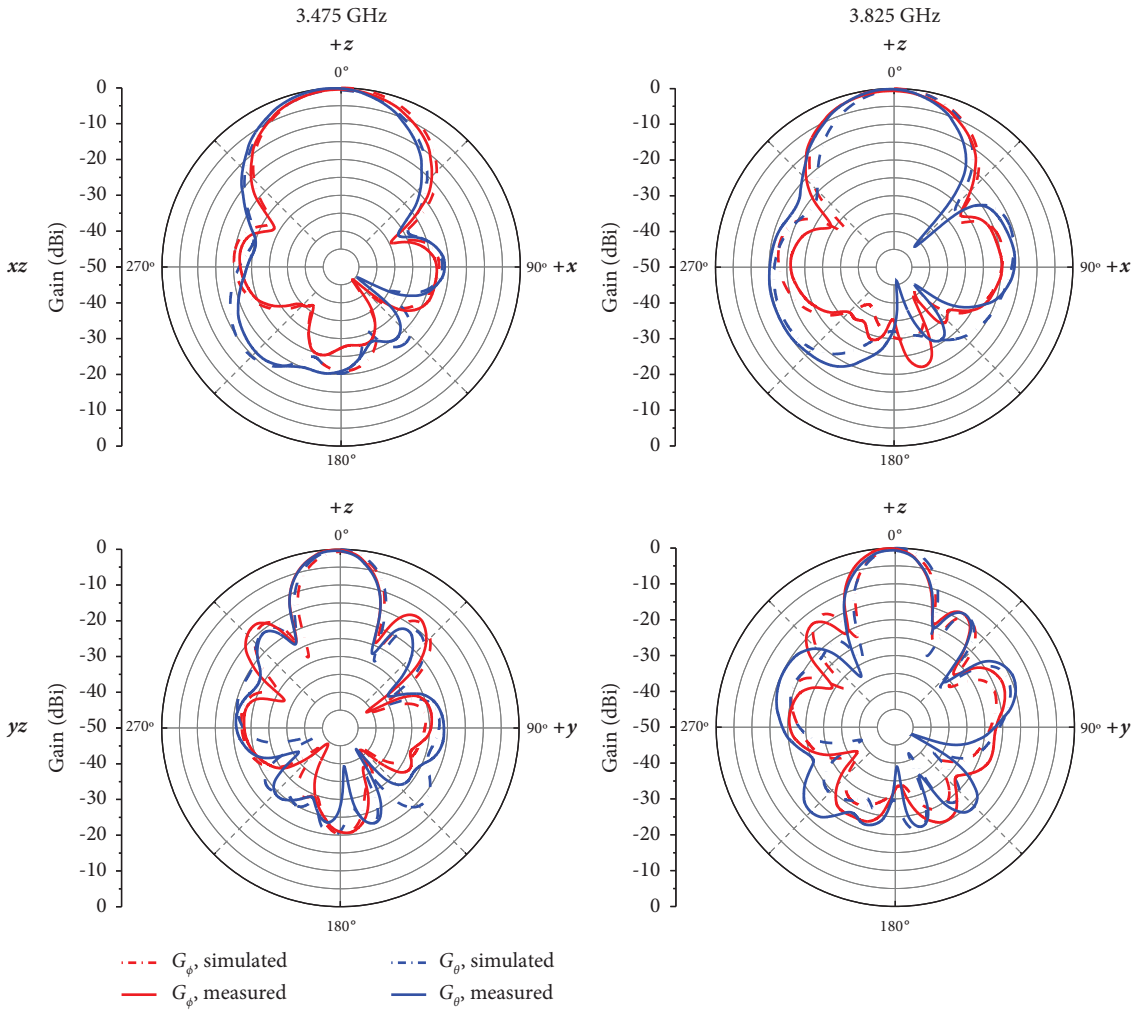

Figure 16: Simulated and measured radiation patterns of the proposed 8-element antenna array at different planes and frequencies.

$$\text{Radiation Efficiency (\%)} = \frac{\text{Gain}}{\text{Directivity}} \times 100. \quad (3)$$

Photos of the antenna unit and arrays as well as the comparison between simulated and measured results, including return losses, gain, radiation efficiency, and radiation patterns are presented with brief discussions as follows.

3.1. Antenna Unit. Figure 7 shows the photo of the proposed antenna and its simulated and measured return loss, gain, and efficiency. The overall dimension is 65 mm × 65 mm × 11.4 mm. As shown in the figure, bandwidth of 10-dB return loss from 3.23 to 3.97 GHz or a fractional bandwidth of 20.6% has been achieved. Compared to simulated data, separation between the lower and higher resonant mode has been enlarged, resulting a degradation of impedance around 3.8 GHz, which could be attributed to the fabrication error of slightly increased substrate spacing owing to PCB warpage, which is in consistent with the parameter study shown in Figure 4. 6.2 dBi gain and 74% efficiency has been achieved in the entire n78 frequency band. The measured peak gain 7.18 dBi and maximum efficiency of 82% around 3.4 GHz has been obtained. Good coherences were also obtained in the radiation patterns, as shown in Figure 8.

3.2. Four-Element Antenna Array. Figure 9 shows the photo of the proposed 4-element antenna array. The overall dimension is 115 mm × 115 mm × 11.4 mm. The simulated and measured return losses are shown in Figure 10. As shown in the figure, bandwidth of 10-dB return loss from 3.22 to 3.92 GHz, or a fractional bandwidth of 19.6% has been achieved. Figure 11 shows that 10.5 dBi gain and 56% efficiency has been achieved in the entire n78 frequency band. Measured peak gain 11 dBi around 3.8 GHz and maximum efficiency of 82% around 3.5 GHz has been obtained. Good coherences were also obtained in the radiation patterns, as shown in Figure 12.

3.3. Eight-Element Antenna Array. Figure 13 shows the photo of the proposed 4-element antenna array. The overall dimension is 115 mm × 215 mm × 11.4 mm. The simulated and measured return loss is shown in Figure 14. As shown in the figure, bandwidth of 10-dB return loss from 3.2 to

Table 2: Comparison of key parameters and performance.

Antenna	Applied design method	Number of radiation elements	Size (mm^3 (λ_0^3))	Edge-to-edge distance, mm (λ_0)	Bandwidth (GHz)	Peak gain (dBi)	Radiation efficiency (%)	Isolation (dB)	Design complexity	Practical applications
[6]	Multiple parasitic patches	4 (2 × 2)	160 × 160 × 3.5 (1.76 × 1.76 × 0.038)	~4 (~0.044)	3.35–3.9510-dB	13.6	—	>20	Low	Scanning phased arrays
[14]	Parasitic strips	4 (2 × 2)	6.4 × 5 × 0.1 (1.29 × 1.01 × 0.020)	~1.2 (~0.24)	57–6310-dB	5.7	—	—	Low	WPAN
[16]	Opposite side feeding	4 (2 × 2)	26 × 16.5 × 0.76 (2.42 × 1.54 × 0.071)	3.8 (0.35)	26.75–29.610-dB	10.35	—	—	Low	LMDS
[28]	EBG, DSG, neutral lines	4 (2 × 2)	46 × 46 × 1.6 (0.58 × 0.58 × 0.020)	8.8 (0.11)	3.1–5.510-dB	9	92(max)	>20	Low	5 G FR1
[29]	Metasurface	4 (2 × 2)	100 × 100 × 38 (1.17 × 1.17 × 0.44)	4.5 (0.053)	3.3–3.715-dB	7.2	90	>25	Low	5 G base stations
[30]	Dielectric cavity	8 (2 × 4), dual pol	101 × 170 × 14 (1.16 × 1.96 × 0.16)	40 (0.46)	3.2–3.915-dB	6.8	—	>40	Low	5 G, MIMO
Proposed antenna	Probe-fed, parasitic element, Wilkinson power divider	1	65 × 65 × 11.4 (0.74 × 0.74 × 0.13)	—	3.23–3.9910-dB	7.18	74	—	Low	5 G FR1 CPE
Proposed 4-element array		4 (2 × 2)	115 × 115 × 11.4 (1.30 × 1.30 × 0.13)	17.9 (0.20)	3.0–3.9210-dB	11	56	>24	Low	5 G FR1 CPE
Proposed 8-element array		8 (2 × 4)	115 × 215 × 11.4 (1.30 × 2.44 × 0.13)	17.9 (0.20)	3.0–3.9910-dB	13.01	50	>20	Low	5 G FR1 CPE

4.0 GHz or a fractional bandwidth of 22.2% has been achieved. Figure 15 shows that a 12 dBi gain and 50% efficiency have been achieved in the entire n78 frequency band. Measured peak gain 13.8 dBi around 3.8 GHz and maximum efficiency of 56% around 3.4 GHz has been obtained. Good coherences were also obtained in the radiation patterns, as shown in Figure 16.

4. Conclusions

A microstrip patch antenna with parasitic element has been proposed to build two antenna arrays of different sizes for CPE ODU applications in the n78 frequency band of 5 G NR FR1. The antenna unit has achieved a bandwidth of 10-dB return loss from 3.23 to 3.29 GHz which fully covered the desired frequency band. 6.2 dBi gain and 74% efficiency have been achieved in the entire n78 frequency band with a peak gain of 7.18 dBi and a maximum efficiency of 82%. Wilkinson power-divider-based feeding networks are used to realize the proposed four-element and eight-element arrays. Rotated antenna units with respect to their feeding points were also proposed to reduce mutual coupling to below −20 dB without increasing the separations between antenna units and overall array sizes. The proposed four-element and eight-element arrays exhibited average gains around 10.5 dBi and 13 dBi, respectively, and more than 10 dB return loss throughout the entire n78 frequency band. The comparison of key parameters and performance for different antennas is listed in Table 2, where λ_0 is the wavelength at the first resonance frequency of respective antenna element in free space. The proposed method is easily extended for the realization of array antennas with element numbers in the powers of 2. For element numbers that are not multiples of 2, n-way Wilkinson power dividers are also available but not as trivial [39]. For large arrays the loss of the transmission line segments in the FR4 substrate will significantly reduce the gain of increasing element numbers, thus low loss substrates must be used instead. The proposed antenna arrays have demonstrated the advantages of simple, low-cost, low profile, as well as high gain characteristics over the entire n78 frequency band, which is potentially applicable to 5 G CPE outdoor unit (ODU)-related devices.

Data Availability

The simulated and measured data used to support the findings of this study are available from the corresponding author upon request.

Conflicts of Interest

The authors declare that they have no conflicts of interestr.

Acknowledgments

The authors would like to acknowledge BWant Co. Ltd. for the help on the experimental verification of the proposed antenna arrays with their automated OTA measurement system. This paper was supported in part by the Ministry of Science and Technology, under Grant MOST 110-2221-E-035-023-.

References

[1] J. Sun, J. Li, and L. Xia, "A dual-polarized magneto-electric dipole antenna for application to n77/n78 band," *IEEE Access*, vol. 7, pp. 161708–161715, 2019.

[2] S. Wi, Y. Lee, and J. Yook, "Wideband microstrip patch antenna with U-shaped parasitic elements," *IEEE Transactions on Antennas and Propagation*, vol. 55, no. 4, pp. 1196–1199, 2007.

[3] H. Satow, E. Nishiyama, and I. Toyoda, "Gain enhancement of a dual feed microstrip array antenna using parasitic elements," in *Proceedings of the 2015 International Symposium on Antennas and Propagation (ISAP)*, pp. 1–4, Hobart, TAS, Australia, November 2015.

[4] D. Wen, D. Zheng, and Q. Chu, "A dual-polarized planar antenna using four folded dipoles and its array for base stations," *IEEE Transactions on Antennas and Propagation*, vol. 64, no. 12, pp. 5536–5542, 2016.

[5] J. Anguera, G. Font, C. Puente, C. Borja, and J. Soler, "Multifrequency microstrip patch antenna using multiple stacked elements," *IEEE Microwave and Wireless Components Letters*, vol. 13, no. 3, pp. 123-124, 2003.

[6] K. D. Xu, J. Zhu, S. Liao, and Q. Xue, "Wideband patch antenna using multiple parasitic patches and its array application with mutual coupling reduction," *IEEE Access*, vol. 6, pp. 42497–42506, 2018.

[7] A. Katyal and A. Basu, "Compact and broadband stacked microstrip patch antenna for target scanning applications," *IEEE Antennas and Wireless Propagation Letters*, vol. 16, pp. 381–384, 2017.

[8] J. Wang, J. Shi, and Q. Cao, "A high-gain broadband stacked patch antenna with finite ground," in *Proceedings of the 2017 Sixth Asia-Pacific Conference on Antennas and Propagation*, pp. 1–3, APCAP, Xi'an, China, October 2017.

[9] V. S. Kraanthi, "High gain circularly polarized stacked patch antenna at c-band for geo satellite telemetry application," in *Proceedings of the 2019 IEEE Indian Conference on Antennas and Propogation*, pp. 1–4, Ahmedabad, India, December 2019.

[10] M. Akbari, M. Farahani, A. R. Sebak, and T. A. Denidni, "A 30GHz high-gain circularly-polarized pattem-steerable antenna based on parasitic patches," in *Proceedings of the 2017 11th European Conference on Antennas and Propagation (EUCAP)*, pp. 3044–3046, Paris, France, March 2017.

[11] K. Lee, J. Oh, and S. Yi, "Stacked microstrip patch antenna array with high-gain and improved thermal-stability for microwave power transmission applications," in *Proceedings of the 2018 Asia-Pacific Microwave Conference (APMC)*, pp. 1432–1434, Kyoto, Japan, November 2018.

[12] M. Saad Khan and F. A. Tahir, "A circularly polarized stacked patch antenna array for tracking applications in S-band," in *Proceedings of the 2015 9th European Conference on Antennas and Propagation (EuCAP)*, pp. 1–4, Lisbon, Portugal, April 2015.

[13] L. Wang, J. Wang, and J. Shi, "Design of 4×4 meandering-fed stacked patch antenna array," in *Proceedings of the 2018 International Workshop on Antenna Technology (iWAT)*, pp. 1–3, Nanjing, China, March 2018.

[14] H. Jin, W. Che, W. Yang, and K.-. Chin, "High-gain 60-GHz patch antenna array using GaN MMIC technology," in *Proceedings of the 2015 IEEE 4th Asia-Pacific Conference on Antennas and Propagation (APCAP)*, pp. 150-151, Bali, Indonesia, July 2015.

[15] M. U. Raza and S. Yan, "Dual band millimeter wave phased array antenna for 5G mobile communications," in *Proceedings*

of the 2020 IEEE 3rd International Conference on Electronic Information and Communication Technology (ICEICT), pp. 247-248, Shenzhen, China, December 2020.

[16] K.-S. Chin, H.-T. Chang, J.-A. Liu, H.-C. Chiu, J. S. Fu, and S.-H. Chao, "28-GHz patch antenna arrays with PCB and LTCC substrates," in *Proceedings of the 2011 Cross Strait Quad-Regional Radio Science and Wireless Technology Conference*, pp. 355–358, Harbin, China, July 2011.

[17] M. Wang et al., "A Ka-band high-gain dual-polarized microstrip antenna array for 5G application," in *Proceedings of the 2019 International Conference on Microwave and Millimeter Wave Technology (ICMMT)*, pp. 1–3, Guangzhou, China, May 2019.

[18] Z. Ling, C. Liu, and H. Li, "Wideband patch antenna array for 5G terminal devices," in *Proceedings of the 2020 IEEE 3rd International Conference on Electronic Information and Communication Technology (ICEICT)*, pp. 610–612, Shenzhen, Chin, November 2020.

[19] D. De, A. Prakash, N. Chattoraj, P. K. Sahu, and A. Verma, "Design and analysis of various Wilkinson power divider networks for L band applications," in *Proceedings of the 2016 3rd International Conference on Signal Processing and Integrated Networks (SPIN)*, pp. 67–72, Noida, India, February 2016.

[20] G. M. Aji, M. A. Wibisono, and A. Munir, "High gain 2.4 GHz patch antenna array for rural area application," in *Proceedings of the 2016 22nd Asia-Pacific Conference on Communications (APCC)*, pp. 319–322, Yogyakarta, August 2016.

[21] J. Xiao, T. Ding, and Q. Ye, "High-gain multilayer patch antenna array," in *Proceedings of the 2020 9th Asia-Pacific Conference on Antennas and Propagation (APCAP)*, pp. 1-2, Xiamen, China, August 2020.

[22] H. Wang, K. E. Kedze, and I. Park, "Microstrip patch array antenna using a parallel and series combination feed network," in *Proceedings of the 2018 International Symposium on Antennas and Propagation (ISAP)*, pp. 1-2, Busan, Korea (South), October 2018.

[23] D. N. Arizaca-Cusicuna, J. Luis Arizaca-Cusicuna, and M. Clemente-Arenas, "High gain 4×4 rectangular patch antenna array at 28GHz for future 5G applications," in *Proceedings of the 2018 IEEE XXV International Conference on Electronics, Electrical Engineering and Computing (INTERCON)*, pp. 1–4, Lima, August 2018.

[24] K.-X. Li, Y.-W. Wu, and Z.-C. Hao, "A 5G millimeter-wave circularly polarized planar antenna array," in *Proceedings of the 2020 9th Asia-Pacific Conference on Antennas and Propagation (APCAP)*, pp. 1-2, Xiamen, China, August 2020.

[25] B. P. A. Mahatmanto and C. Apriono, "Planar microstrip array antenna with rectangular configuration fed with Chebyshev power distribution for C-band satellite application," in *Proceedings of the 2019 IEEE International Conference on Innovative Research and Development (ICIRD)*, pp. 1–4, Jakarta, Indonesia, June 2019.

[26] L. Chen, W. Yang, W. Che, and Q. Xue, "High-isolation dual-polarized patch antenna array," in *Proceedings of the 2020 IEEE MTT-S International Microwave Workshop Series on Advanced Materials and Processes for RF and THz Applications (IMWS-AMP)*, pp. 1–3, Suzhou, China, July 2020.

[27] S. Mohammadi-Asl, J. Nourinia, C. Ghobadi, and M. Majidzadeh, "Wideband compact circularly polarized sequentially rotated array antenna with sequential-phase feed network," *IEEE Antennas and Wireless Propagation Letters*, vol. 16, pp. 3176–3179, 2017.

[28] A. A. Megahed, M. Abdelazim, E. H. Abdelhay, and H. Y. M. Soliman, "Sub-6 GHz highly isolated wideband MIMO antenna arrays," *IEEE Access*, vol. 10, pp. 19875–19889, 2022.

[29] J. Guo, F. Liu, L. Zhao, Y. Yin, G.-L. Huang, and Y. Li, "Metasurface antenna array decoupling designs for two linear polarized antennas coupled in H-plane and E-plane," *IEEE Access*, vol. 7, pp. 100442–100452, 2019.

[30] M. Li, X. Chen, A. Zhang, and A. A. Kishk, "Dual-polarized broadband base station antenna backed with dielectric cavity for 5G communications," *IEEE Antennas and Wireless Propagation Letters*, vol. 18, no. 10, pp. 2051–2055, 2019.

[31] H. Ş. Savcı, "A four element stringray-shaped MIMO antenna system for UWB applications," *Micromachines*, vol. 14, no. 10, pp. 1944–1963, 2023.

[32] A. K. Singh and M. Ranjan Tripathy, "M-shaped ultra wide band monopole antenna for TVWS CPE," in *Proceedings of the 2018 5th International Conference on Signal Processing and Integrated Networks (SPIN)*, pp. 240–243, Noida, India, February 2018.

[33] A. K. Singh and M. R. Tripathy, "Planar trapezoidal monopole antenna for TVWS CPE," in *Proceedings of the 2018 3rd International Conference for Convergence in Technology (I2CT)*, pp. 1–3, Mangalore, India, April 2018.

[34] N. I. M. Elamin and T. A. Rahman, "2-Element slot meander patch antenna system for LTE-WLAN customer premise equipment," in *Proceedings of the 2015 IEEE-APS Topical Conference on Antennas and Propagation in Wireless Communications (APWC)*, pp. 993–996, Turin, Italy, September 2015.

[35] J.-H. Lu, B.-M. Chen, and W.-R. Chuang, "Design of dual-band slot antenna array for 5G sub-6 GHz CPE," in *Proceedings of the 2021 International Symposium on Antennas and Propagation (ISAP)*, Taipei, Taiwan, November 2021.

[36] R. Zhang, Z. Yi, Y. Chen, L. Zhu, H. Jin, and G. Yang, "A hybrid antenna system for 5G-WLAN customer premise equipment (CPE) application," in *Proceedings of the 2019 International Applied Computational Electromagnetics Society Symposium-China (ACES)*, pp. 1-2, Nanjing, China, August 2019.

[37] X. Tang, H. Chen, B. Yu, W. Che, and Q. Xue, "Bandwidth enhancement of a compact dual-polarized antenna for Sub-6G 5G CPE," *IEEE Antennas and Wireless Propagation Letters*, vol. 21, no. 10, pp. 2015–2019, 2022.

[38] R. B. Waterhouse, "Design of probe-fed stacked patches," *IEEE Transactions on Antennas and Propagation*, vol. 47, no. 12, pp. 1780–1784, 1999.

[39] D. M. Pozar, *Microwave Engineering*, Wiley, New York, NY, USA, 2011.

[40] Bwant Co Ltd, "CATR automated OTA measurement system," https://www.bw-ant.com/en/product.html.

[41] J. Kulkarni, N. Kulkarni, and A. Desai, "Development of "H-Shaped" monopole antenna for IEEE 802.11a and HIPERLAN 2 applications in the laptop computer," *International Journal of RF and Microwave Computer-Aided Engineering*, vol. 30, no. 7, 2020.

[42] J. Kulkarni, "Multi-band printed monopole antenna conforming bandwidth requirement of GSM/WLAN/WiMAX standards," *Progress In Electromagnetics Research Letters*, vol. 91, pp. 59–66, 2020.

[43] J. Kulkarni and C. Y. D. Sim, "Wideband CPW-fed oval-shaped monopole antenna for wi-fi5 and wi-fi6 applications," *Progress in Electromagnetics Research C*, vol. 107, pp. 173–182, 2021.

[44] J. S. Kulkarni, "Design and development of ultra-thin monopole antenna for WLAN and WiMAX operations in the next-generation laptop computer," in *Proceedings of the 2019 International Conference on Radar, Antenna, Microwave, Electronics, and Telecommunications (ICRAMET)*, pp. 79–83, Tangerang, Indonesia, October 2019.